Model for Calcium Binding to γ-Carboxyglutamic Acid Residues of Proteins: Crystal Structure of Calcium α-Ethylmalonate†

Alan Zell,* Howard Einspahr, and Charles E. Bugg

Departments of Microbiology and Biochemistry, Institute of Dental Research, and Comprehensive Cancer Center, University of Alabama at Birmingham, University Station, Birmingham, Alabama 35294
Received May 4, 1984; Revised Manuscript Received August 30, 1984

ABSTRACT: The crystal structure of a Ca^{2+} salt of α-ethylmalonic acid was determined from three-dimensional X-ray diffraction data. The dicarboxylate anion represents the functional side chain of γ-carboxyglutamic acid (Gla) residues, which are implicated as essential calcium-binding ligands in a variety of proteins. The α-ethylmalonate ion chelates the Ca^{2+} ion in a bidentate manner that involves an O atom from each of the two malonate carboxylate groups. This type of binding arises from the constrained arrangement of carboxylate ligands in the malonate group and may be of significance to the calcium-binding properties of Gla-containing sites in proteins. The Ca^{2+}–malonate chelation forms a six-membered ring, which is stabilized by interactions that are consistent with the preferred stereochemistries of both calcium–carboxylate and metal–malonate complexes. No other interactions are observed between Ca^{2+} ions and α-ethylmalonate ions that depend upon the malonate juxtaposition of two carboxylate groups. The potential for this type of binding distinguishes Gla residues from the monocarboxylate residues, aspartate and glutamate, and confers a novel calcium-chelation ability upon Gla-containing sites in proteins.

Calcium(2+) ions play principal roles in the regulation of biological processes. In many of these processes, complex formation with proteins is implicated in the molecular mechanism of Ca^{2+} action. One class of such calcium-binding proteins is distinguished by the presence of a modified amino acid residue, γ-carboxyglutamic acid (Gla) (Stenflo et al., 1974), incorporated through a posttranslational, vitamin K dependent, microsomal carboxylation of glutamate residues (Esmon et al., 1975a). This class includes zymogens of the blood clotting pathway [Jackson & Nemerson (1980) and references therein], as well as proteins isolated from bone matrix (Hauschka et al., 1975; Price et al., 1976), dentin (Linde et al., 1980), chorioallantoic membrane (Tuan & Scott, 1977), and a variety of ectopic calcifications (Lian et al., 1976). Studies of Ca^{2+} binding to decarboxylated forms of Gla-containing proteins (Stenflo & Ganrot, 1973; Esnouf & Prowse, 1977; Hauschka & Carr, 1982) indicate that the presence of Gla residues is required for these proteins to interact with Ca^{2+} ions [with apparent dissociation constants of 10^{-3}–10^{-4} M (Nelsestuen, 1976; Hauschka & Gallop, 1977)].

Direct interaction between Gla side chains and Ca^{2+} ions is suggested by NMR spectroscopic studies of ^{43}Ca and lanthanide complexes of Gla-rich peptides (Robertson et al., 1978; Furie et al., 1979). The virtually invariant positions of the Gla residues in the sequences of a number of Gla-containing proteins of bone [Hauschka & Carr (1982) and references cited therein] and in the sequences of the NH_2-terminal portions of the Gla-containing plasma proteins [Davie (1980) and references cited therein] suggest the importance of the spatial relationship of the Gla residues in Gla-containing proteins. In prothrombin and a Gla-containing protein from bone, spectral analyses suggest that Ca^{2+} binding involving Gla residues induces a reversible coil-to-helix structural transition (Bloom & Mann, 1978; Hauschka & Carr, 1982) of similar magnitude to those seen in the intracellular calcium-binding proteins troponin C (Murray & Kay, 1972) and calmodulin (Klee, 1977). Coordination of Ca^{2+} ions to Gla residues of Gla-containing proteins appears to be responsible for a number of the functional properties of these proteins, including the capacity of the plasma clotting factors to bind to phospholipid dispersions (Esmon et al., 1975b) and the capacity of the bone Gla-containing proteins to adsorb to calcium phosphate mineral surfaces (Hauschka et al., 1975).

The calcium-binding properties conferred on proteins by Gla residues are not well understood in structural terms. However, several lines of evidence, including accumulated crystallographic data from a variety of calcium complexes, indicate that the geometrical arrangements of ligands limit the types of sites that can bind Ca^{2+} ions with significant affinity. Therefore, it seems likely that Gla residues contribute to calcium-binding sites on proteins by providing ligand groups in orientations that are particularly favorable for Ca^{2+} chelation. In order to understand more about the geometries of Ca^{2+}–Gla interactions, we undertook the crystallographic study of a Ca^{2+} salt of the functional side-chain analogue of Gla residues, α-ethylmalonic acid.

Experimental Procedures

Clear platelike crystals of the calcium salt of α-ethylmalonic acid were grown at room temperature by slow evaporation of a filtered solution of approximately 1:1 molar quantities of the acid and calcium bromide in water, adjusted to pH 7.4 by addition of sodium hydroxide. Oscillation and Weissenberg photographs showed $2/m$ diffraction symmetry and indicated the monoclinic crystal system. Space group $P2_1/c$ was uniquely indicated by the systematic absence of reflections of the type $0k0$, k odd, and $h0l$, l odd. Three-dimensional diffraction intensity data were collected within a temperature range of 20–22 °C from a single crystal of approximate dimensions 1.1 × 1.1 × 0.1 mm on an automated four-circle diffractometer by use of nickel-filtered copper radiation. Measurements were made for each of the 1086 symmetry-independent reflections of $2\theta < 128°$. Three reflections that were remeasured peri-

† This work was supported by National Institutes of Health Grants DE-02670 and Ca-13148. H.E. is the recipient of NIH Research Career Development Award DE-00106.

* Address correspondence to this author at the Comprehensive Cancer Center, University of Alabama at Birmingham.

0006-2960/85/0424-0533$01.50/0

Table I: Crystal Data (Cu Kᾱ)[a]

stoichiometry	$CaC_5O_4H_6$
formula units/unit cell (Z)	4
crystal system	monoclinic
space group	$P2_1/c$
a (Å)	11.003 (2)
b (Å)	6.595 (1)
c (Å)	9.723 (2)
β (deg)	110.14 (1)
ρ_{calcd} (g cm^{-3})	1.706
ρ_{obsd} (g cm^{-3})	1.71 (3)
calcd linear absorption coeff (μ) (cm^{-1})	78.5
no. of independent observations ($I > 0$)	1021

[a] Estimated standard deviations (ESD's) in quantities reported here and elsewhere in the manuscript are represented parenthetically and have the order of magnitude of the least significant digit of the quantity to which they are appended. ESD's in a, b, c, and β are based on a least-squares analysis.

odically during data collection to monitor crystal decay showed no significant fluctuations. Precise estimates of the unit-cell parameters were obtained by a least-squares analysis of the observed 2θ values (Cu Kᾱ, λ = 1.5418 Å; $T \simeq 21$ °C) of 14 medium-resolution reflections. Crystal density was measured at room temperature by flotation in a mixture of ethylene bromide, carbon tetrachloride, and benzene. Pertinent crystal data are listed in Table I.

Of the 1086 unique reflections measured, 65 had scan counts below background level and were assigned intensity values of 0.0. The raw intensity data were reduced to net intensities and assigned variances, $\sigma^2(I)$, on the basis of counting statistics. An additional intensity-dependent term, $(0.03S)^2$, where S = scan count, was added to $\sigma^2(I)$ to account for measured uncertainity introduced by instrumental instability. Analytical corrections for Lorentz and polarization effects and for absorption were made to the net intensities and their variances. Transmission factors, evaluated by numerical integration (computer program ORABS; Wehe et al., 1962), ranged from 0.50 to 0.89. The data were then put on an absolute scale according to Wilson (1942) statistics.

A trial structure was obtained by conventional Patterson and Fourier methods. These trial coordinates, together with an absolute scale factor (k) and individual isotropic thermal parameters, were refined by a full-matrix least-squares analysis that minimized $\sum w(|F_o| - |F_c|)^2$, where $w = 1/\sigma^2(F_o)$ and where $|F_o|$ and $|F_c|$ are the square roots of the observed and calculated intensities (Frenz, 1978). X-ray atomic scattering factors, and anomalous dispersion corrections to the factors, were taken from Tables 2.2B and 2.3.1 of *International Tables for X-ray Crystallography* (1974).

Five of the six hydrogen atoms were located by a difference Fourier synthesis calculated after several cycles of least-squares refinement. The remaining hydrogen atom, attached to the methyl carbon atom, was assigned an approximate position on the basis of expected bonding geometry. Final cycles of refinement included the scale factor, positional and anisotropic thermal parameters for the non-hydrogen atoms, positional and isotropic thermal parameters for the hydrogen atoms, and an isotropic secondary extinction parameter. At convergence, the conventional R value ($\sum||F_o| - |F_c||/\sum|F_o|$) considering all unique data measured is 0.060, and the estimated goodness-of-fit ($[\sum w(|F_o| - |F_c|)^2/v]^{1/2}$, where v = number of observations minus number of parameters refined) is 1.96. In the last cycle of refinement, no parameter shifted more than $^1/_{50}$th of its estimated standard deviation (ESD). A final difference electron density map calculated from the refined model showed no peaks or troughs exceeding 0.25 e/Å^3 in magnitude.

Table II: Atomic Parameters and Their Estimated Standard Deviations[a]

atom	x	y	z	U_{iso}, U_{eq} (Å^2)
Ca	0.51369 (7)	0.5145 (1)	−0.30790 (7)	0.0166 (2)
O1	0.5820 (2)	0.3321 (4)	−0.0778 (2)	0.019 (1)
O2	0.6089 (2)	0.3154 (2)	0.1603 (2)	0.020 (1)
O3	0.6420 (2)	0.8987 (4)	0.0506 (2)	0.021 (1)
O4	0.6533 (2)	0.7434 (4)	−0.1446 (2)	0.017 (1)
C1	0.6333 (3)	0.3905 (5)	0.0535 (4)	0.016 (1)
C2	0.7339 (3)	0.5617 (6)	0.0845 (4)	0.021 (1)
C3	0.6741 (3)	0.7476 (5)	−0.0084 (4)	0.017 (1)
C4	0.8527 (4)	0.4846 (6)	0.0514 (5)	0.030 (1)
C5	0.9173 (5)	0.3063 (9)	0.1465 (6)	0.061 (2)
H1	0.760 (3)	0.597 (6)	0.182 (3)	0.02 (1)
H2	0.825 (4)	0.442 (6)	−0.052 (4)	0.03 (1)
H3	0.911 (3)	0.602 (6)	0.062 (4)	0.03 (1)
H4	0.993 (5)	0.248 (9)	0.123 (6)	0.08 (2)
H5	0.938 (5)	0.331 (9)	0.253 (6)	0.10 (2)
H6	0.860 (5)	0.194 (8)	0.128 (5)	0.07 (2)

[a] Values of x, y, and z are in fractions of the unit-cell edges, a, b, and c, respectively. Isotropic thermal parameters, $U_{iso} = \overline{u^2}$ = mean-square amplitude of vibration, are shown for hydrogen atoms. Equivalent isotropic thermal factors for the non-hydrogen atoms are given by $U_{eq} = (1/3)(U_{11} + U_{22} + U_{33} + 2U_{12}\cos\gamma + 2U_{13}\cos\beta + 2U_{23}\cos\alpha)$, where the U_{ij} values define the thermal ellipsoids in terms of mean-square amplitudes of vibration. The atom numbering scheme is defined in Figure 1.

An analysis of the final residuals $[||F_o| - |F_c||/\sigma(F_o)]$ vs. $(\sin\theta)/\lambda$ revealed that, of the 22 reflections with $|\Delta|/\sigma \geq 5$, 21 (with $|\Delta|/\sigma$ values ranging up to 11) lie in the $(\sin\theta)/\lambda$ interval 0.553–0.568 Å^{-1}. A check of scan and background counts for reflections in this interval suggests that an unexplained systematic variation in background scattering is responsible for the concentration of large residuals. To test the effects that these reflections might have exerted on our refined model, the 18 reflections with the largest residuals were removed from the data set, and the structure was again refined to convergence. No parameter shifted more than 1 ESD.

Results

Final estimates of atomic coordinates and isotropic thermal vibration parameters (or their equivalents) are listed in Table II. Tables of observed and calculated structure factors and of anisotropic atomic thermal parameters are available as supplementary material (see paragraph at end of paper regarding supplementary material). ESD's in positional parameters are approximately 0.0007 Å for the Ca^{2+} ion, 0.002 Å for O atoms, 0.004 Å for C atoms, and 0.05 Å for H atoms, on the basis of the least-squares analysis. The conformation of the anion along with bond lengths and angles is presented in Figure 1.

Sites at which the α-ethylmalonate anion binds crystallographically related Ca^{2+} ions are depicted in Figure 2. The Ca^{2+} ion is surrounded by an eight-membered coordination polyhedron formed by O atoms from seven carboxylate groups contributed by six symmetry-related anions (Figure 3). Three different modes of interaction comprise the coordination scheme. Four of the six anions bind the Ca^{2+} ion in a unidentate fashion that involves a single carboxylate O atom. One anion chelates the Ca^{2+} ion in a bidentate manner via both O atoms of a single carboxylate group. The sixth α-ethylmalonate ion also chelates the Ca^{2+} ion in a bidentate manner, but this chelation involves a single O atom from each of the two carboxylate groups of the anion; this interaction is referred to as the malonate chelation. The geometries of the unidentate and bidentate calcium–carboxylate interactions observed in this structure are in good agreement with the preferred geometries of these modes of binding,which are discussed in a

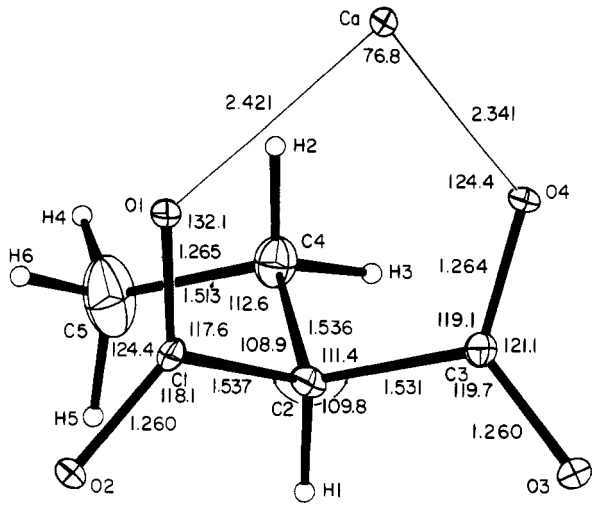

FIGURE 1: The asymmetric unit of the calcium α-ethylmalonate crystal structure, showing bond lengths (Å) and bond angles (°) that involve non-hydrogen atoms. Non-hydrogen atoms are represented as ellipsoids of thermal vibration, scaled to include 50% probability density. Hydrogen atoms are represented by spheres of arbitrary volume. Estimated standard deviations (ESD's) in bond distances are approximately 0.002, 0.003, and 0.004 Å for Ca–O, C–O, and C–C bonds, respectively. ESD's in bond angles are approximately 0.2°. All figures were prepared by use of the computer program ORTEP (Johnson, 1965).

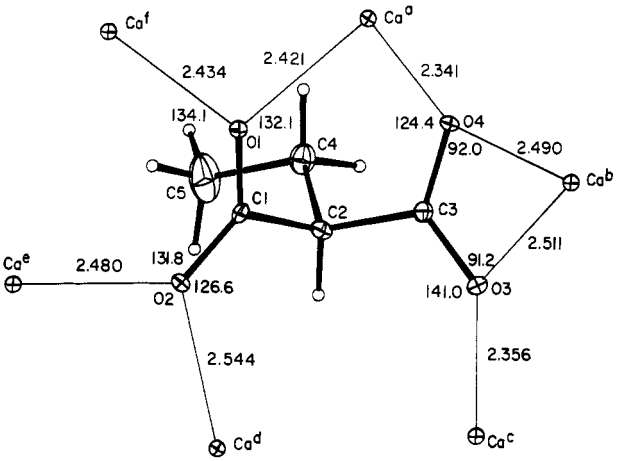

FIGURE 2: Cationic environment of the α-ethylmalonate ion in the crystal, showing the modes by which the anion coordinates to Ca^{2+} ions. Atom representation and ESD's in bond distances and angles are as stated in the caption to Figure 1. Ca^{2+} ions are related by symmetry operations denoted in superscript by the letters a–f as follows: (a) x, y, z; (b) $1-x, {}^1/_2+y, {}^{-1}/_2-z$; (c) $x, {}^3/_2-y, {}^1/_2+z$; (d) $1-x, 1-y, -z$; (e) $x, {}^1/_2-y, {}^1/_2+z$; (f) $1-x, {}^{-1}/_2+y, {}^{-1}/_2-z$.

recent survey by Einspahr & Bugg (1981). Both unidentate and bidentate modes are found to involve Ca–O distances between 2.2 and 2.75 Å. Unidentate coordinations, due to relative lack of constraint, show the greatest variability: a bimodal distribution of Ca–O–C angles with peaks at 110–140 and 150–170° and deviations of Ca^{2+} ions from carboxylate planes that range up to 2.4 Å. Bidentate chelations, due to confinement by interactions with both O atoms of the carboxylate group, show the most restricted range: Ca–O–C angles between 80 and 100° and deviations of Ca^{2+} ions from carboxylate planes of less than 1.0 Å.

The malonate chelation, which involves an O atom from each of the two carboxylate groups of the anion, is of special interest. Unlike the unidentate and bidentate interactions, it is a type of Ca^{2+} coordination that is not possible with monocarboxylate amino acid side chains (viz., those of aspartate and glutamate). It is shown in isolation in Figure 1 and with

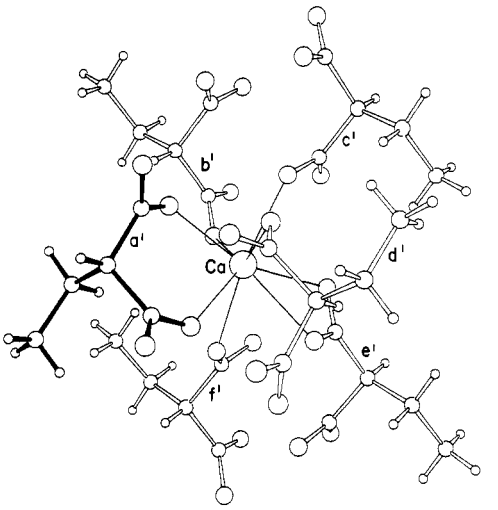

FIGURE 3: Anionic environment of the Ca^{2+} ion in the crystal. Atoms are represented by spheres of arbitrary radii, scaled relative to atomic number. Anions are related by symmetry operations denoted by the letters a′–f′ as follows: (a′) $x, {}^1/_2-y, {}^1/_2+z$; (b′) $x, -1+y, z$; (c′) $1-x, -y, -z$; (d′) $1-x, {}^{-1}/_2+y, {}^1/_2-z$; (e′) $1-x, 1-y, -z$; (f′) x, y, z. The position of the Ca^{2+} ion is given by $x, {}^1/_2-y, {}^1/_2+z$. The anion at position $x, {}^1/_2-y, {}^1/_2+z$, illustrating the malonate mode of calcium chelation, is highlighted by blackened bonds.

the other calcium–carboxylate interactions in Figure 3. This chelation forms a six-membered ring that includes the Ca^{2+} ion, along with atoms O1, C1, C2, C3, and O4. Atoms O1, C1, C3, and O4 of the ring are coplanar within 0.062 (4) Å, while the Ca^{2+} ion and atom C2 are situated 0.575 (1) Å and −0.706 (4) Å, respectively, on opposite sides of the O1, C1, C3, O4 least-squares plane. The ring appears to be relatively free of internal strain, as no ring bond angles deviate significantly from preferred values and no nonbonded interactions with distances at van der Waals limits are evident. The two Ca–O coordination bonds of the ring, considered individually, have geometries that are consistent with observed unidentate geometries cited above. The Ca–O–C angles are 124 and 132°, and the Ca^{2+} ion deviates from the two carboxylate planes by 1.07 and 1.74 Å. The Ca–O distances are, respectively, the shortest and third shortest of the eight Ca–O bonds in this structure and are at the lower extreme of the distribution of Ca–O distances observed in calcium–carboxylate complexes (Einspahr & Bugg, 1981).

The malonate chelation seems to be a favored mode of interaction of the malonate group with alkali metal, alkaline earth, lanthanide, and transition metal ions [see, for examples, Soriano-Garcia & Rao (1983), Duc et al. (1978), Briggman & Oskarsson (1977, 1978), Lis & Matuszewski (1979), Butler & Snow (1976), Post & Trotter (1974), and Hansson (1973a,b)]. Of the approximately 45 independent metal–malonate complexes that have been studied crystallographically, roughly three-fourths form this six-membered chelate ring. In many of these other metal–malonate salts, the chelation is favored in spite of considerable angle strain imposed at the tetrahedral C2 atom of the malonate group by distortion of the C1–C2–C3 valence angle. Deviations by as much as 16° from the tetrahedral value are observed in several of these compounds and appear to be the result of the relatively flattened conformations assumed by the chelate rings (Matsumoto & Kuroya, 1972; Briggman & Oskarsson, 1978; Duc et al., 1978; Soriano-Garcia & Parthasarathy, 1978; Pajunen & Pajunen, 1980). Such conformations place the two malonate carboxylate groups nearly coplanar with one another and with the plane through the carbon backbone of the malonate group, requiring C–C–C angle opening to relieve the resultant

overcrowding of the proximal O atoms. In the free malonic acids, which do not have this chelate ring system as a constraint on the relative orientation of the two carboxyl groups, the most common conformation places one carboxyl group approximately coplanar with, and the other approximately perpendicular to, the C1, C2, C3 plane (Goedkoop & MacGillavry, 1957; Lepore et al., 1975, 1976), avoiding C–C–C angle distortion. In calcium α-ethylmalonate, O···O repulsion is minimized [d_{O1-O4} = 2.957 (3) Å] by twist of both carboxylate groups (by 57 and −73°, respectively) out of the C1, C2, C3 plane, and no C–C–C angle strain is evident [angle C1–C2–C3 = 109.8 (2)°].

Discussion

In the crystal structure of calcium α-ethylmalonate, we observe three modes of interaction between Ca^{2+} ions and the carboxylate groups of the α-ethylmalonate ion: (i) a unidentate mode in which a Ca^{2+} ion interacts with only one carboxylate O atom, (ii) a bidentate chelation mode in which a Ca^{2+} ion interacts with both O atoms of a single carboxylate group, and (iii) a malonate chelation mode in which a Ca^{2+} ion interacts with two O atoms, one from each of the two carboxylate groups of a single α-ethylmalonate ion, to form a six-membered chelate ring. The first two modes of binding are typical of the interactions between Ca^{2+} ions and individual carboxylate groups observed in a wide variety of crystalline calcium complexes and thus reflect properties of monocarboxylate chemistry. The latter mode of interaction, though, is clearly dependent upon the dicarboxylate nature of the α-ethylmalonate ion and is thus directly a property of the malonate group itself rather than of its component carboxylate groups. The potential for this latter type of chelation distinguishes the Gla residue from the monocarboxylate functional residues aspartate and glutamate. We propose that this mode of interaction, the malonate chelation, is of significance to the biological activity of Gla residues in protein calcium-binding sites and may represent a functional role of the γ-carboxylation process. The malonate chelation appears to be a preferred mode of interaction, occurring frequently in other metal–malonate complexes. As discussed above, the observed chelate is a six-membered ring system that seems to be relatively strain free. The calcium–carboxylate interactions within this ring, considered individually, form with geometries that lie within the range of those observed in crystalline calcium complexes (Einspahr & Bugg, 1981).

The malonate chelation in this crystal structure is the only interaction between the Ca^{2+} ion and the α-ethylmalonate ion that involves both carboxylate groups of the same anion. The availability of four O atoms in the malonate group, however, suggests the possibility of tri- or quadridentate Ca^{2+} ion chelation by this group and its derivatives (Sperling et al., 1978; Furie et al., 1979). We have examined models of such chelates and find them to be highly unlikely, since they require calcium–carboxylate interactions that are inconsistent with those observed in other crystal structures. In Ca^{2+} chelates involving both O atoms of a carboxylate group, deviations of the Ca^{2+} ion from the carboxylate plane do not exceed 1 Å and Ca–O–C angles do not fall outside the narrow range of 80–100° (Einspahr & Bugg, 1981). In contrast, tridentate chelation would force the Ca^{2+} ion to lie considerably (>2 Å) out of the plane of the carboxylate group that donates both O atoms and would result in Ca–O–C coordination angles of approximately 70° with this carboxylate group. Likewise, quadridentate chelation requires deviations of the Ca^{2+} ion by more than 2 Å from both carboxylate planes of the malonate group and results in Ca–O–C angles of approximately 60°. A survey of the approximately 45 other metal complexes of malonate derivatives that have been studied crystallographically does not reveal any instances of tri- or quadridentate metal–malonate chelates. Nor are any multidentate chelation patterns involving a carboxylate group as a bidentate donor found in Ca^{2+} complexes of carboxylate derivatives (Einspahr & Bugg, 1981). Therefore, we feel that the malonate chelation pattern depicted in Figure 1 is the one most likely to be involved in interactions between Ca^{2+} ions and Gla residues of proteins.

Calcium-binding sites on proteins generally involve several ligands. The geometrical arrangements of the component ligands with respect to the Ca^{2+} ion appear to be major factors in stabilizing complexes between Ca^{2+} ions and proteins. Accumulated crystallographic data from a variety of calcium complexes reveal favored calcium–ligand coordination geometries, which differ among the various types of ligands [Einspahr & Bugg (1980, 1981, 1983) and references therein]. In contrast, coordination numbers and types of ligands appear to be similar at both strong and weak calcium-binding sites in proteins (Einspahr & Bugg, 1983; Kretsinger & Nelson, 1976), and uncharged ligands (e.g., water molecules and carbonyl groups) can make major contributions to both types of sites. The malonate chelation, which we observe in the title structure, represents a favorable arrangement of ligands for binding Ca^{2+} ions that may contribute to calcium-binding sites in proteins that contain Gla residues.

Acknowledgments

We thank Mary Ann Jones for assistance in preparation of the manuscript and drawings.

Supplementary Material Available

A table of anisotropic thermal parameter estimates for non-hydrogen atoms and a table of observed and calculated structure factor amplitudes (11 pages). Ordering information is given on any current masthead page.

Registry No. Ca, 7440-70-2; calcium α-ethylmalonate, 94137-06-1; γ-carboxyglutamic acid, 53445-96-8.

References

Bajaj, S. P., Price, P. A., & Russell, W. A. (1982) *J. Biol. Chem. 257*, 3726–3731.

Bloom, J. W., & Mann, K. G. (1978) *Biochemistry 17*, 4430–4438.

Briggman, B., & Oskarsson, Å. (1977) *Acta Crystallogr., Sect. B B33*, 1900–1906.

Briggman, B., & Oskarsson, Å. (1978) *Acta Crystallogr., Sect. B B34*, 3357–3359.

Butler, K. R., & Snow, M. R. (1976) *J. Chem. Soc., Dalton Trans.*, 251–258.

Davie, E. W. (1980) in *Vitamin K Metabolism and Vitamin K-Dependent Proteins* (Suttie, J. W., Ed.) pp 3–7, University Park Press, Baltimore, MD.

Duc, G., Faure, R., & Loiseleur, H. (1978) *Acta Crystallogr., Sect. B B34*, 2115–2118.

Einspahr, H., & Bugg, C. E. (1980) *Acta Crystallogr., Sect. B B36*, 264–271.

Einspahr, H., & Bugg, C. E. (1981) *Acta Crystallogr., Sect. B B37*, 1044–1052.

Einspahr, H., & Bugg, C. E. (1983) *Met. Ions Biol. Syst. 17*, 51–97.

Esmon, C. T., Sadowski, J. A., & Suttie, J. W. (1975a) *J. Biol. Chem. 250*, 4744–4748.

Esmon, C. T., Suttie, J. W., & Jackson, C. M. (1975b) *J. Biol. Chem. 250*, 4095–4099.

Esnouf, M. P., & Prowse, C. V. (1977) *Biochim. Biophys. Acta 490*, 471–476.
Frenz, B. A. (1978) *Computing in Crystallography* (Schenk, H., Olthof-Hazekamp, R., van Koningsveld, H., & Bassi, G. C., Eds.) pp 64–71, Delft University Press, Delft, The Netherlands.
Furie, B. C., Blumenstein, M., & Furie, B. (1979) *J. Biol. Chem. 254*, 12521–12530.
Goedkoop, J. A., & MacGillavry, C. H. (1957) *Acta Crystallogr. 10*, 125–127.
Hansson, E. (1973a) *Acta Chem. Scand. 27*, 2813–2826.
Hansson, E. (1973b) *Acta Chem. Scand. 27*, 2827–2840.
Hauschka, P. V., & Gallop, P. M. (1977) in *Calcium Binding Proteins and Calcium Function* (Wasserman, R. H., et al., Eds.) pp 338–347, Elsevier, New York.
Hauschka, P. V., & Carr, S. A. (1982) *Biochemistry 21*, 2538–2547.
Hauschka, P. V., Lian, J. B., & Gallop, P. M. (1975) *Proc. Natl. Acad. Sci. U.S.A. 72*, 3925–3929.
International Tables for X-ray Crystallography (1974) Vol. IV, pp 71–151, Kynoch Press, Birmingham, England.
Jackson, C. M., & Nemerson, Y. (1980) *Annu. Rev. Biochem. 49*, 765–811.
Johnson, C. K. (1965) *Oak Ridge Natl. Lab.*, [*Rep.*] *ORNL (U.S.) ORNL-3794* (revised).
Klee, C. B. (1977) *Biochemistry 16*, 1017–1024.
Kretsinger, R. H., & Nelson, D. J. (1976) *Coord. Chem. Rev. 18*, 29–124.
Lepore, U., Lepore, G. C., & Ganis, P. (1975) *Acta Crystallogr., Sect. B B31*, 2874–2876.
Lepore, U., Lepore, G. C., & Ganis, P. (1976) *Cryst. Struct. Commun. 5*, 29–30.
Lian, J. B., Skinner, M., Glimcher, M. J., & Gallop, P. M. (1976) *Biochem. Biophys. Res. Commun. 71*, 1207–1213.
Linde, A., Bhown, M., & Butler, W. T. (1980) *J. Biol. Chem. 255*, 5931–5942.
Lis, T., & Matuszewski, J. (1979) *Acta Crystallogr., Sect. B B35*, 2212–2214.
Matsumoto, K., & Kuroya, H. (1972) *Bull. Chem. Soc. Jpn. 45*, 1755–1759.
Murray, A. C., & Kay, C. M. (1972) *Biochemistry 11*, 2622–2626.
Nelsestuen, G. L. (1976) *J. Biol. Chem. 251*, 5648–5656.
Pajunen, A., & Pajunen, S. (1980) *Acta Crystallogr., Sect. B B36*, 2425–2428.
Post, M. L., & Trotter, J. (1974) *J. Chem. Soc., Dalton Trans.*, 1922–1925.
Price, P. A., Otsuka, A. S., Poser, J. W., Kristaponis, J., & Raman, N. (1976) *Proc. Natl. Acad. Sci. U.S.A. 73*, 1447–1451.
Robertson, P., Jr., Hiskey, R. G., & Koehler, K. A. (1978) *J. Biol. Chem. 253*, 5880–5883.
Soriano-Garcia, M., & Parthasarathy, R. (1978) *J. Chem. Soc., Perkin Trans. 2*, 667–670.
Soriano-Garcia, M., & Rao, S. N. (1983) *Acta Crystallogr., Sect. C: Cryst. Struct. Commun. C39*, 850–852.
Sperling, R., Furie, B. C., Blumenstein, M., Keyt, B., & Furie, B. (1978) *J. Biol. Chem. 253*, 3898–3906.
Stenflo, J., & Ganrot, P. O. (1973) *Biochem. Biophys. Res. Commun. 50*, 98–104.
Stenflo, J., Fernlund, P., Egan, W., & Roepstorff, P. (1974) *Proc. Natl. Acad. Sci. U.S.A. 71*, 2730–2733.
Tuan, R. S., & Scott, W. A. (1977) *Proc. Natl. Acad. Sci. U.S.A. 74*, 1946–1949.
Wehe, D. J., Busing, W. R., & Levy, H. A. (1962) *Oak Ridge Natl. Lab.*, [*Rep.*] *ORNL-TM (U.S.) ORNL-TM-229*.
Wilson, A. J. C. (1942) *Nature (London) 150*, 151–152.